Geomechanics and Engineering, *Vol. 29, No. 6 (2022) 615-626*
https://doi.org/10.12989/gae.2022.29.6.615

A simple creep constitutive model for soft clays based on volumetric strain characteristics

G. Chen[1a], J.G. Zhu[1b], Z. Chen[1c] and W.L. Guo*[2]

[1]*Minist Educ Geomech & Embankment Engn, Key Lab, Hohai Univ, Nanjing 210098, Jiangsu, China*
[2]*Geotech Engn Dept, Nanjing Hydraul Res Inst, Nanjing 210024, Jiangsu, China*

(Received January 22, 2022, Revised May 2, 2022, Accepted May 3, 2022)

Abstract. The soft clays are widely distributed, and one of the prominent engineering problems is the creep behavior. In order to predict the creep deformation of soft clays in an easier and more acceptable way, a simple creep constitutive model has been proposed in this paper. Firstly, the triaxial creep test data indicated that, the strain-time (ε-t) curve showing in the ε-lg$t$ space can be divided into two lines with different slopes, and the time referring to the demarcation point is named as t_{EOP}. Thereafter, the strain increments occurred after the time t_{EOP} are totally assumed to be the creep components, and the elastic and plastic strains had occurred before t_{EOP}. A hyperbolic equation expressing the relationship between creep volumetric strain, stress and time is proposed, with several triaxial creep test data of soft clays verifying the applicability. Additionally, the creep flow law is suggested to be similar with the plastic flow law of the modified Cam-Clay model, and the proposed volumetric strain equation is used to deduced the scaling factor for creep strains. Therefore, a creep constitutive model is thereby established, and verified by successfully predicting the creep principal strains of triaxial specimens.

Keywords: clay; constitutive model; creep; flow rule; triaxial test

1. Introduction

The soft clays that generally refers to the clays with high moisture content, high compressibility, low bearing capacity, and low permeability are most widely applied in engineering, which is of great significance for the safety maintenance of buildings and structures. Thus, the characteristics of soft clays are concerned by engineers, especially creep. The creep process of soft clays reflects the variation law of strain with time under constant stress. Many engineering incidents are known to be caused by creep (Vialov 1987). For example, because the iconic Leaning Tower of Pisa is built on a soft foundation, the soft soil causes excessive creep deformation over time, resulting in uneven foundation settlement and tower leaning. A reinforced concrete viaduct erected on a clay slope in Switzerland was significantly distorted due to soft soil creep and had to be dismantled. Furthermore, the famous dam in France exacerbated the displacement of the dam foundation due to the creep of the soft soil, leading in the dam's disintegration. Therefore, in engineering applications, a creep model that can represent reasonable well creep of soft clays is required. Only by establishing a realistic creep model can the flow characteristics of soil particles be objectively reflected and the prediction accuracy of soil creep be improved, resulting in fewer engineering accidents (Hessam and Mohammad 2012, Zhao *et al*. 2018).

Scholars have presented several creep models in recent years (Thu 2015, Thu 2017, Alexander 2021), and the empirical model has attracted much attention because of its minimal number of parameters, unambiguous physical meaning of parameters, and easy formulations (Chen *et al.* 2014, Mataic *et al*. 2016, Liu *et al.* 2019). The classical three parameters model, Singh-Mitchell model, was presented (Singh and Mitchell 1968) from the laboratory triaxial drained creep test results. The model describes the relationship of stress with strain by the exponential function and the relationship of strain with time by the power function. The model parameters, including A_r, α, m, can be determined easily, and the physical meaning of material parameters is considered to be rational and intuitive. The model, however, applies to creep tests with shear stress levels ranging from 20% to 80%.

Other scholars (Mesri *et al*. 1981, Lin and Wang 1998) improved Singh-Mitchell model. Mesri *et al*. (1981), for example, proposed alternative combinations of the hyperbolic stress-strain and either power strain-time. The predictions of the model are lower at beginning of creep, the strain rate larger over time, which deviates greatly from the test data. Zhu *et al*. (2006) improved the Singh-Mitchell creep model of soft clays based on Mesri model and a series of laboratory triaxial creep tests of soft clays of the Pearl River Delta, and it was discovered that the model parameters' values vary with drainage conditions.

According to the time line theory, the logarithmic creep equation proposed by Yin and Graham (1989, 1994, 1996) includes only two parameters ψ/V and t_0 that can be

*Corresponding author, Ph.D., Senior engineer
E-mail: wlguo@nhri.cn
[a]Ph.D.
E-mail: gechenhhu@163.com
[b]Professor
[c]Ph.D.

ISSN: 2005-307X (Print), 2092-6219 (Online)

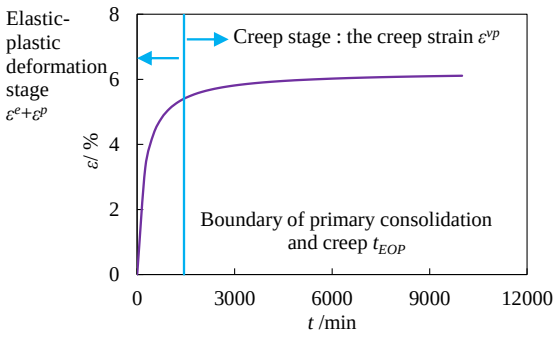

Fig. 1 Sketch of the second assumption

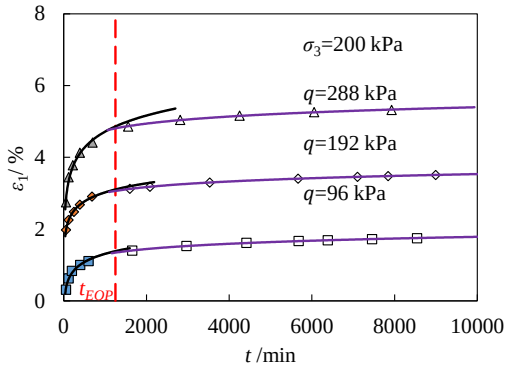

(a) Curves of ε-t

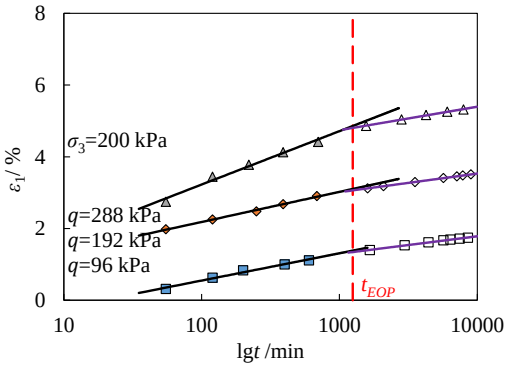

(b) Curves of ε-ln$t$

Fig. 2 Calculated vertical strain with time for creep of Daishan soft clays

obtained by fitting creep test data. The model is convenient and practical, but with increasing t, the strain increases infinitely, which may be impossible. In order to overcome this limitation, a new nonlinear logarithmic function, which is essentially a hyperbolic function, was proposed (Yin and Graham 1999, Yin and Zhu 1999). The deformation of soils can be accurately described, but the starting point of creep calculation is still controversial. Furthermore, other researchers updated the EVP model by taking into account the creep limit (Thu *et al*. 2015, Chen *et al.* 2021). and test data and simulation confirm the efficiency and accuracy of the upgraded models in predicting creep of soft clays.

In conclusion, despite the fact that there have been several research on the empirical creep model, hyperbolic form was adopted in most improvements. Clearly, hyperbolic function is more reasonable to describe the creep stain of soft clays. Therefore, a hyperbolic volumetric creep model is proposed and verified based on a large number of laboratory test results. Compared with the Singh-Mitchell model, the proposed model captures the test data of soft clays reasonably well for shear stress levels less than 20%.

2. The calculation starting point of creep strain

The difficulty of establishing creep constitutive model of soils is how to determine the starting point of creep. At present, there are two main assumptions for the selection of the starting point of creep calculation. One assumption is that creep begins to happen when the load is applied, in other words, creep happens in the whole stage of consolidation. The total strain is the sum of an elastic strain and a creep strain, and can be written as Eq. (1).

$$\varepsilon = \varepsilon^e + \varepsilon^{tp} \tag{1}$$

Where ε is the total strain. ε^e is the elastic strain. ε^{tp} is the creep strain of the whole stage of consolidation. The limitation of this assumption is that under constant total stress, the pore water pressure in the primary consolidation stage changes continuously, which resulted in the effective stress changing. According to the concept of creep, creep occurs under constant the effective stress, so the deformation of soils during this period cannot be called creep in a strict sense.

Another assumption is to separate the primary consolidation and secondary consolidation compression. The secondary consolidation compression used to be referred to as creep compression occurring after the excess pore water pressure dissipates to zero. The whole deformation process of soils is divided into elastic-plastic deformation unrelated to time and creep deformation related to time, and can be written as Eq. (2).

$$\varepsilon = \begin{cases} \varepsilon^e + \varepsilon^p, T \le t_{EOP} \\ \varepsilon^e + \varepsilon^p + \varepsilon^{vp}, T > t_{EOP} \end{cases} \tag{2}$$

Where ε_p is the plastic strain. ε^{vp} is the creep strain. T is the time of deformation. t_{EOP} is the time of primary consolidation, as shown in Fig. 1.

The second assumption can overcome the shortcoming of effective stress change, but the end time of primary consolidation is not easy to determine, which is affected by soil thickness, shear stress level, temperature and other external conditions. Therefore, some scholars (Hu 2013) take the inflection point of curve in the plane of ε-t under single-stage loading as the completion time of primary consolidation. This approach is simple to operate, which is also used to determine the starting point of creep calculation in this paper.

Taking soft soils of Daishan as an example, its physical and mechanical properties are listed in Table 1. According to the *Geotechnical Test Method Standard* (Cai *et al*. 2019), the specimen is put into the oedometer for oedometer test, and the loads are taken 50, 100, 200, 400, 800, 1600kPa, the consolidation time is 7 days, and the deformation value is read according to the specification, and the curves of ε-t are

Table 1 Basic physical and mechanical parameters of. Daishan clays

G_s	w/%	ρ/(g/cm3)	w_l/%	w_p/%
2.73	33.3	1.82	37.5	21.7

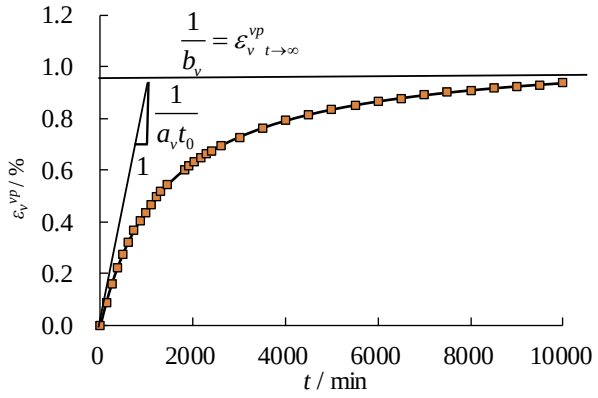

Fig. 3 Sketch of the physical meanings of two parameters

shown in Fig. 2(a). It should be observed that the inflection point of the curve is not easy to determine. The strain-time (ε-t) curve showing in the ε-lg$t$ space can be divided into two lines sharply with different slopes, as shown in Fig. 2(b), and thus the intersection of two lines in the ε-lg$t$ space is used as the starting point of creep. This paper mainly studies the creep period, so, the creep starting point is denoted as zero time point in the ε^{vp}-t space.

Fig. 2 shows it is little difference about time of primary consolidation of Daishan soft soils under the same confining pressure and different effective shear stresses. The reason for this phenomenon is that the specimens, 80 mm in height, are thin, resulting in faster drainage speed. The primary consolidation time is shorter and closer under different effective shear stresses. However, in engineering application, primary consolidation time of soft soils with thickness of several meters or even ten meters may be quite various under different stress states.

3. A hyperbolic equation for the volumetric creep strain with time

3.1. The proposal of volumetric creep equation

Based on the results of a large number of triaxial drainage consolidation creep tests, the variation trend of strain-time curve is analyzed, and a hyperbolic volumetric creep equation (3) is proposed as follows.

$$\varepsilon_v^{vp} = \frac{t}{\alpha_v t_0 + \beta_v t} \tag{3}$$

Where ε_v^{vp} is the volumetric strain of soft clays after the creep starting for a period of time t. t_0(=1440 min) is adopted to allow dimensionless equation. α_v and β_v are two soil mechanical parameters, which can be obtained from triaxial drainage consolidation creep tests. Physical meaning and determination of the parameters will be discussed in detail as following.

From Eq. (3), if the time is infinite, the limiting volumetric strain is the following, as Eq. (4)

$$\varepsilon_{v\ t\to\infty}^{vp} = \frac{1}{\beta_v} \tag{4}$$

From Eq. (4), if $t\to\infty$, $1/\beta_v$ is equal to the limiting volumetric strain. Parameter β_v is directly related to the limiting volumetric strain. The former equals to the reciprocal of the latter, as shown in Fig. 3.

By differentiating Eq. (3) with respect to t, the volumetric creep strain rate is expressed as Eq. (5).

$$\frac{d\varepsilon_v^{vp}}{dt} = \frac{\alpha_v t_0}{(\alpha_v t_0 + \beta_v t)^2} \tag{5}$$

From Eq. (5), if time is zero, the initial volumetric strain rate is Eq. (6).

$$\dot{\varepsilon}_{v\to 0}^{vp} = \frac{1}{\alpha_v t_0} \tag{6}$$

$\dot{\varepsilon}_{v\to 0}^{vp}$ is the initial tangent slope in the plane of ε_v^{vp}-t, its physical meaning is the initial volumetric creep strain rate. Parameter α_v is related to the initial volumetric creep strain rate. $\alpha_v t_0$ equals to the reciprocal of the latter, as shown in Fig. 3.

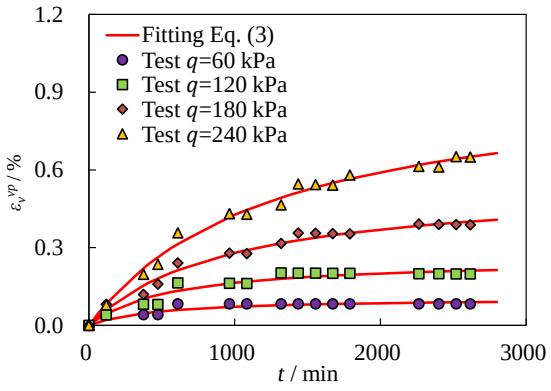

(a) σ_3=150 kPa

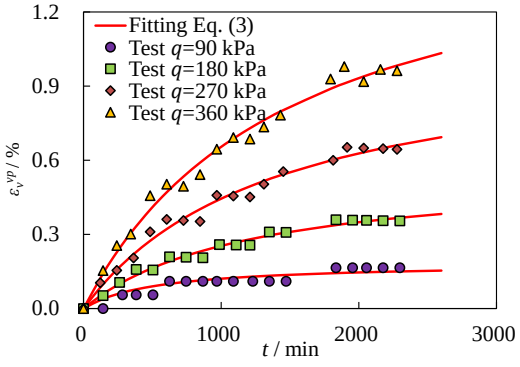

(b) σ_3=200 kPa

Fig. 4 Measured and calculated volumetric strain with time for creep of Cangzhou clay

Table 2 Basic physical and mechanical parameters of. Cangzhou clays (Liu 2020)

G_s	w/%	e_0/%	ρ/(g/cm^3)	ρ_d/(g/cm^3)
2.65	30	1.1	2.12	1.63

Table 3 Results of curve fitting by Eq. (3) of Cangzhou clays

σ_3 (kPa)	q (kPa)	p (kPa)	R^2	α_v	β_v
150	60	170	0.97	3.11	9.41
	120	190	0.96	1.52	3.89
	180	210	0.96	1.22	1.83
	240	230	0.95	0.91	1.04
200	90	230	0.94	2.06	5.42
	180	260	0.97	1.48	1.78
	270	290	0.99	0.91	0.94
	360	320	0.93	0.63	0.62

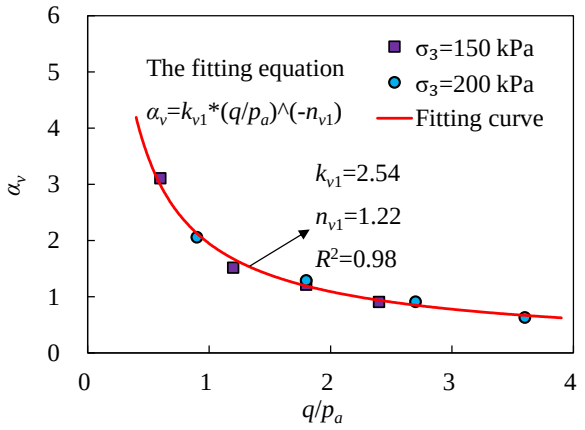

Fig. 5 Relationship of parameter α_v versus q/p_a

Cangzhou coastal remolded clays is taken as an example (Liu 2020). The fitting results of Eq. (3) are illustrated, and its physical and mechanical properties are listed in Table 2. Hyperbolic formula is used to fit the results of triaxial CD creep test with confining pressure of 150 kPa and 200 kPa, respectively, as shown in Fig. 4. Conclusion can be drawn as followings from the figure: the development law of volumetric creep can be well described by Eq. (3), and the fitting values are in good agreement with the experimental value.

Furthermore, the soil mechanical parameters α_v and β_v and correlation coefficient R^2 of Cangzhou coastal clays fitted by Eq. (3) are given, such as Table 3. It is seen from Table 3 that the fitting correlation coefficients are above 0.9. Implying that it is reasonable to describe the volumetric creep of Cangzhou coastal clays by Eq. (3).

3.2 Parameters determination

It is observed from Table 2 that parameters α_v and β_v are different under different confining pressures and different shear stress states, that is, two parameters are closely related to the stress state of soil. The author found that parameter α_v

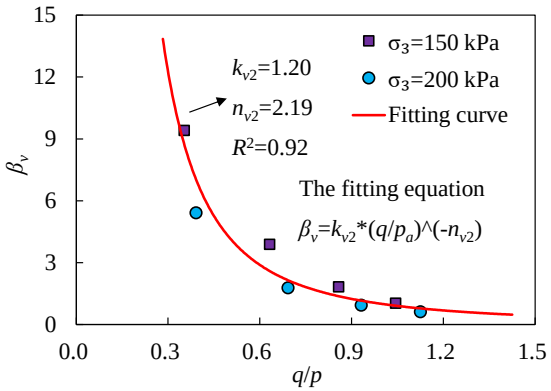

Fig.6 Relationship of parameter β_v versus q/p

is related to the effective shear stress q and parameter β_v is related to the effective stress ratio q/p, and the rule has universal applicability. In order to get dimensionless equation, the standard atmospheric pressure p_a is used, p_a=100 kPa. Using the data in Table 2, the two parameters α_v and β_v are plotted in the plane of α_v -q/p_a and β_v -q/p, respectively, as shown in Fig. 5 and Fig. 6.

It is seen from Fig. 5 that α_v decreases with increasing q/p_a. It is found that the points can be fitted well by a power Eq. (17), as shown in Fig. 5. The test points are slightly scattered, but the curve tendency is clearly seen. The squared-R is equal to 0.96, indicating good curve fitting in different shear stress states. The equation of the fitted curve could be expressed as Eq. (7)

$$\alpha_v = k_{v1}\left(\frac{q}{p_a}\right)^{-n_{v1}} \tag{7}$$

Where q is the effective shear stress. In triaxial tests, $q=\sigma_1-\sigma_3$. k_{v1} and n_{v1} are non-dimensional soil mechanical parameters. From Fig. 5, the two parameters, k_{v1} and n_{v1} can be determined.

Similarly, it is seen from Fig. 6 that the more q/p, the lower β_v. It is found that the relationship of β_v versus q/p_a could be best fitted by a power function relation curve, as shown Fig. 6. The correlation coefficient R^2 is 0.93, that implies a good curve fitting in different stress ratios of q/p. The equation of the fitted curve could be expressed as Eq. (8).

$$\beta_v = k_{v2}\left(\frac{q}{p}\right)^{-n_{v2}} \tag{8}$$

Where p is the effective mean normal stress. In triaxial tests, $p=(\sigma_1+\sigma_2+\sigma_3)/3$. k_{v2} and n_{v2} are non-dimensional soil mechanical parameters. From Fig. 6, the two parameters, k_{v2} and n_{v2} can be determined.

Substituting Eqs. (7) and (8) into Eq. (3) results in Eq. (9), which is the final expression of volumetric creep strain a under general stress state.

$$\varepsilon_v^{vp} = \frac{t}{k_{v1}\left(\frac{q}{p_a}\right)^{-n_{v1}} t_0 + k_{v2}\left(\frac{q}{p}\right)^{-n_{v2}} t} \tag{9}$$

There are four parameters k_{v1}, n_{v1}, k_{v2} and n_{v2}. They are calculated by Eq. (9), k_{v1}=2.54, n_{v1}=1.22, k_{v2}=1.20 and n_{v2}=2.19.

3.3 Validation of empirical equation

To check the validity of Eq. (9), taking Hong Kong marine deposits as an example (Zhu 2000), physico-mechanical properties of soils are listed in Table 4. Triaxial drainage creep tests were carried out under different confining pressures and shear stresses, as shown in Table 5. In this paper, the data at confining pressure of 400 kPa are used to calculate the model parameters, and then the experimental data at confining pressure of 200 kPa are used to verify Eq. (9).

The calculated results under confining pressure of 400 kPa and different shear stress levels from Eq. (9) are compared to the test data, as shown in Fig. 7. It is seen that the fitting value is significantly greater than the experimental value only when the shear stress is 495.4 kPa, whereas the fitting results are ideal under other stress states.

The parameters of Hong Kong marine deposits are k_{v1}=12.27, n_{v1}=0.65, k_{v2}=1.61 and n_{v2}=0.55.

The predicted results of different shear stress levels using the obtained parameters from Eq. (9) are compared to the test data, as shown in Fig. 8. It is observed that the curves of the proposed equation agree well with the test data, indicating that Eq. (9) has good applicability to describe the volumetric creep of soft clays.

Table 4 Basic physical and mechanical parameters of Hong Kong marine deposits (Zhu 2000)

G_s	w/%	e_0/%	w_l/%	w_p/%
2.66	48.3	1.216	60	28

Table 5 Creep test scheme of Hong Kong marine deposits (Zhu 2000)

reference	σ_3/kPa	q/kPa				
Hong Kong marine deposits	200	98	158.1	28		Model validation
	400	117.1	261.6	495.4	639.9	Parameter solution

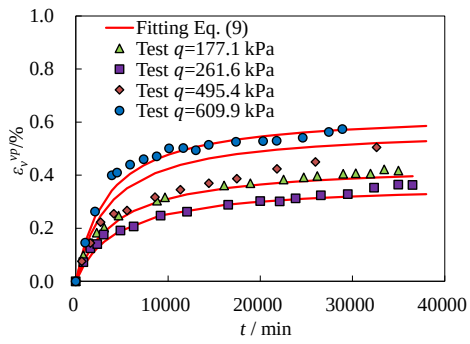

Fig. 7 Measured and calculated volumetric strain with time for creep of Hong Kong marine deposits (σ_3=400 kPa)

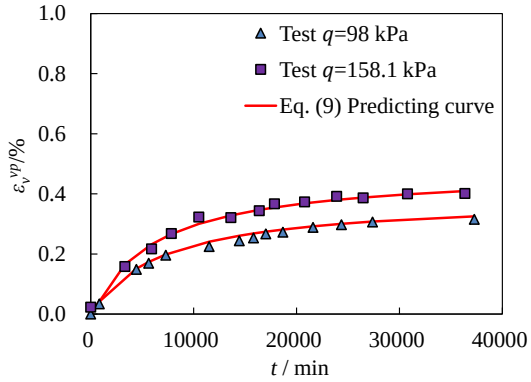

Fig. 8 Measured and predicted volumetric strain with time for creep of Hong Kong marine deposits (σ_3=200 kPa)

In order to further verify the general rationality of Eq. (9), the triaxial drainage test data of soft soils in different regions in China are analyzed. The parameters obtained and the fitting correlation coefficients R^2 are shown in Table 6. Table 6 draws that the coefficient of determination R^2 for the correlation between the test data and predictions are all above 0.9, indicating good curve fitting. The rationality of Eq. (9) is verified.

4. Creep constitutive model

4.1 The proposal of constitutive model

The total incremental strain $d\varepsilon_{ij}$ under general stress state is the sum of an elastic incremental strain $d\varepsilon_{ij}^{e}$, a plastic incremental strain $d\varepsilon_{ij}^{p}$ and a creep incremental strain $d\varepsilon_{ij}^{vp}$, and can be written as Eq. (10).

$$d\varepsilon_{ij} = d\varepsilon_{ij}^{e} + d\varepsilon_{ij}^{p} + d\varepsilon_{ij}^{vp} \tag{10}$$

The elastic strain increment can be derived from the generalized Hooke's law (Derivation is shown in the Appendix A.), and can be written as Eq. (11)

$$d\varepsilon_{ij}^{e} = \frac{1+\mu}{3(1-2\mu)}\frac{\kappa}{1+e_0} p d\sigma_{ij} - \frac{\mu}{(1-2\mu)}\frac{\kappa}{1+e_0} dp\delta_{ij} \tag{11}$$

Where μ is Poisson ratio. σ_{ij} represents the stress value under general stress state. δ_{ij} is a Kronecker symbol, when i=j, δ_{ij}=1, otherwise 0. e_0 is initial void ratio. κ is the slope of the reloading curve after the rebound of the isotropic consolidation test in e-ln$p$ plane.

The plastic strain increment Eq. (12) can be obtained from the modified Cam-Clay model(MCC).

$$d\varepsilon_{ij}^{p} = d\chi\frac{dg}{d\sigma_{ij}} = \frac{\lambda-\kappa}{1+e_0} \left\{\frac{M^2p^2-q^2}{M^2p^2+q^2}\frac{\delta_{ij}}{3p} + \frac{3(\sigma_{ij}-p\delta_{ij})}{M^2p^2+q^2}\right\} \left(dp + \frac{2pq}{M^2p^2-q^2}dq\right) \tag{12}$$

Table 6 The parameters and the fitting correlation coefficient R^2 of soft soils of different regions in China

Soils	k_{v1}	n_{v1}	k_{v2}	n_{v2}	R^2
Soft soil of Zhuhai (Hu 2013)	26.47	1.55	2.04	4.18	0.98
Dalian IMT clays (Zhen *et al*. 2019)	11.00	1.43	1.43	-0.04	0.96
Soft soil of Cangzhou (Liu 2020)	2.54	1.22	1.20	2.19	0.99
HongKong marine deposits (Zhu 2000)	12.27	0.65	1.61	0.55	0.91
Pearl River Delta clays (Zhu *et al*. 2006)	0.46	0.84	0.098	1.13	0.91
Soft soil of Guangdong (Chen *et al*. 2007)	0.41	1.17	0.22	1.19	0.99
Shantou to Jieyang high-speed soft foundation (Dong 2007)	1.23	0.80	0.11	1.69	0.96

Where λ is slope of the loading curve of the isotropic consolidation test in *e*-ln*p* plane

There is a plastic potential surface in the study of plastic strain rate. Similarly, there is a flow surface Q in the study of creep deformation. Similar to the flow rule proposed by Perzyna (1966), the components of creep strain are described by Eq. (13).

$$\frac{d\varepsilon_{ij}^{vp}}{dt} = dS\frac{\partial Q}{\partial \sigma_{ij}} \tag{13}$$

Where Q is the creep strain rate flow surface function. dS is the creep scaling function.

It is assumed that the Q in Eq. (13) have the same form as the elliptic yield surface function of the MCC model, that is, Q=f. Eq. (13) becomes Eq. (14).

$$\frac{d\varepsilon_{v}^{vp}}{dt} = dS\frac{\partial Q}{\partial p} = dS\frac{\lambda-\kappa}{1+e_0}\frac{1}{p}\frac{M^2p^2-q^2}{M^2p^2+q^2} \tag{14}$$

By differentiating Eq. (9) with respect to t, volumetric creep stain rate is described Eq. (15).

$$\frac{d\varepsilon_{v}^{vp}}{dt} = \frac{k_{v1}(\frac{q}{p_a})^{-n_{v1}}t_0}{\left[k_{v1}(\frac{q}{p_a})^{-n_{v1}}t_0 + k_{v2}(\frac{q}{p})^{-n_{v2}}t\right]^2} \tag{15}$$

t can be obtained from Eq. (9), and is given as Eq. (16).

$$t = \frac{\varepsilon_{v}^{vp}k_{v1}(\frac{q}{p_a})^{-n_{v1}}}{1-\varepsilon_{v}^{vp}k_{v2}(\frac{q}{p})^{-n_{v2}}}t_0 \tag{16}$$

The creep scaling function can be derived by combining Eqs. (14)-(16), and is written as Eq. (17).

$$dS = \frac{\left[1-\varepsilon_{v}^{vp}k_{v2}(\frac{q}{p})^{-n_{v2}}\right]^2}{\left[k_{v1}(\frac{q}{p_a})^{-n_{v1}}t_0\right]}\frac{(1+e_0)(M^2p^2+q^2)p}{(\lambda-\kappa)(M^2p^2-q^2)} \tag{17}$$

Eq. (17) is substituted into Eq. (13). The final creep increment under general stress state can be obtained as Eq. (18).

$$\begin{aligned} d\varepsilon_{ij}^{vp} &= dS\frac{dg}{d\sigma_{ij}}dt = dS\left(\frac{\partial g}{\partial p}\frac{\partial p}{\partial \sigma_{ij}} + \frac{\partial g}{\partial q}\frac{\partial q}{\partial \sigma_{ij}}\right)dt \\ &= \frac{\left[\frac{\delta_{ij}}{3} + \frac{3p(\sigma_{ij}-p\delta_{ij})}{M^2p^2-q^2}\right]\left[1-\varepsilon_{v}^{vp}k_{v2}(\frac{q}{p})^{-n_{v2}}\right]^2}{\left[k_{v1}(\frac{q}{p_a})^{-n_{v1}}t_0\right]}dt \end{aligned} \tag{18}$$

Final creep constitutive model is obtained combining Eqs. (11), (12), (18) and (10) (Derivation is shown in the Appendix B.).

The time parameter t_0 and the initial void ratio e_0 of this constitutive model are known. As described above, t_0=1440min, e_0 can be obtained from survey data. Thus there are actually eight parameters in the constitutive model: Parameters M, λ, κ and μ, related to elastic-plastic n_{v1} and n_{v2}, related to creep deformation, are obtained by deformation, are obtained by laboratory conventional triaxial test and compression test data. Parameters k_{v1}, k_{v2}, laboratory triaxial creep test, as shown in the 3.2 section.

4.2 Validation of constitutive model

Calculation of elastic-plastic strain by the MCC model, its applicability to soft clays has been verified in relevant literature (Roscoe and Burland 1968), and creep strain increment thus verified in this paper. The creep starting point is denoted as zero time point in the ε^{vp}-t space. To check the validity of Eq. (18), triaxial drainage creep tests of Zhuhai clays were carried out under different confining pressures and shear stresses. Triaxial drainage creep test data fitting from Eq. (9), the parameters of Zhuhai clays are k_{v1}=26.47, n_{v1}=1.55, k_{v2}=2.04 and n_{v2}=4.18.

The predicted results of major principal strain and minor principal strain using the obtained parameters and relative tress under confining pressure of 200 kPa and different shear stress levels are compared to the test data, as shown in Fig. 9.

Fig. 9 shows the predicted values agree well with the experimental values under various stress states. Indicate that the creep constitutive model has good applicability to describe the volumetric creep of soft clays. It is found that the fitting values of major principal strain are significantly greater than the experimental value only when σ_3=200 kPa, q=264 kPa. The reason for the result may be that the flow

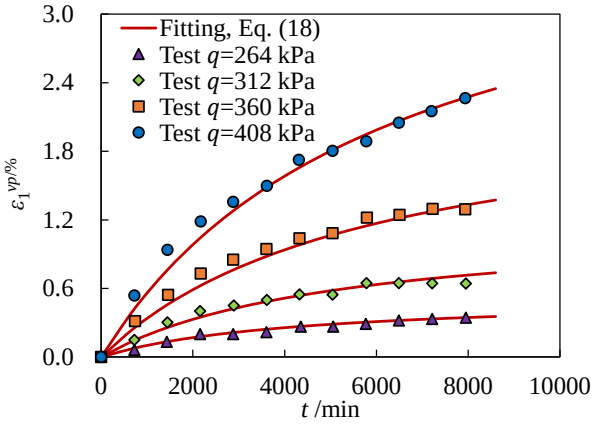

(a) Major principal strain of Zhuhai clays

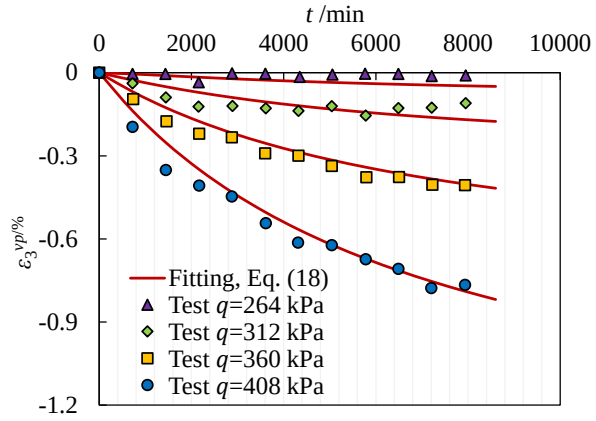

(b) Minor principal strain of Zhuhai clays

Fig. 9 Zhuhai clays σ_3=200 kPa

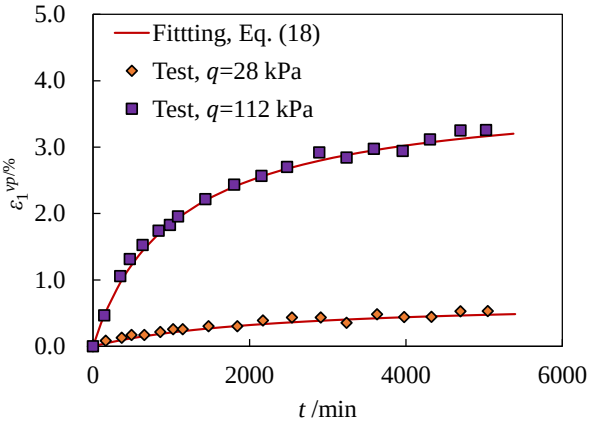

(a) Major principal strain of Guangdong clays

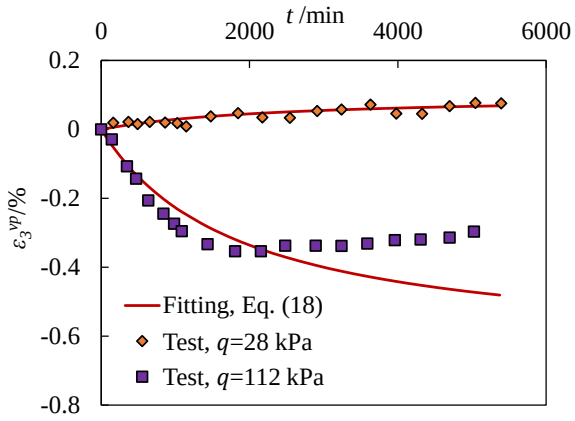

(b) Minor principal strain of Guangdong clays

Fig. 10 Guangdong clays σ_3=100 kPa

surface equation in creep stage is a little unreasonable to use the yield surface equation of the MCC model for reference. Therefore, the flow surface function in creep stage needs to be further studied.

Furthermore, triaxial drainage creep tests of Guangdong clays were carried out under different confining pressures and shear stresses. Triaxial drainage creep test data fitting from Eq. (9), the parameters of Guangdong clays are k_{v1}=0.41, n_{v1}=1.17, k_{v2}=0.22 and n_{v2}=1.19. Taking the creep data when the confining pressure is 100 kPa as an example, the parameters and related stress are used in Eq. (18) to fit data points in Fig. 10.

For major principal strain, it can be observed from Fig. 10 that the fitting curves using Eq. (18) are in good agreement with test points under various stress states. Indicate that the creep constitutive model has good applicability, but, for minor principal strain, the predictions deviates from the experimental data. Especially, when the stress level is high, with the passage of time, the predictions are larger, and the predicted trend is different from the test data. The predictions gradually increases whereas the experimental value first increases but then decreases. It is possible that under high vertical pressure, the soil becomes more and more dense with the passage of loading time, as shown in Fig. 11, which leads to the decrease of deformation.

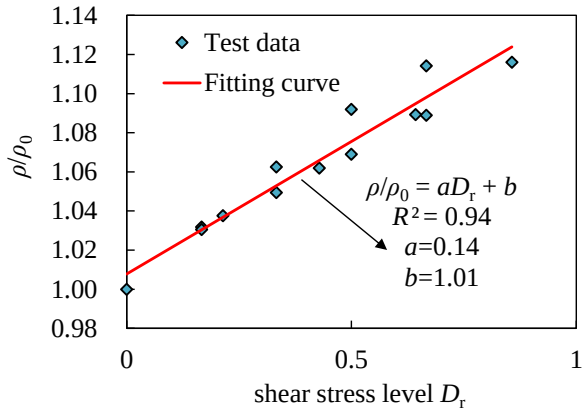

Fig. 11 Curve between density and shear stress levels (Liu 2020)

It is found that the points can be fitted well by a line from Fig 11, as shown in Fig. 5. Eq. (19) can be used to illustrate fitted lines. Fig. 11 shows that density increases with increasing shear stress level D_r. The shear expansion of soft soil is slightly enhanced with the increase of density. After the density reaching a certain degree, that is, the shear expansion rate being greater than the compression rate, volumetric strain of clays transitions from shear contraction to shear expansion. The hyperbolic model can only describe the situation of single increase or single decrease, which

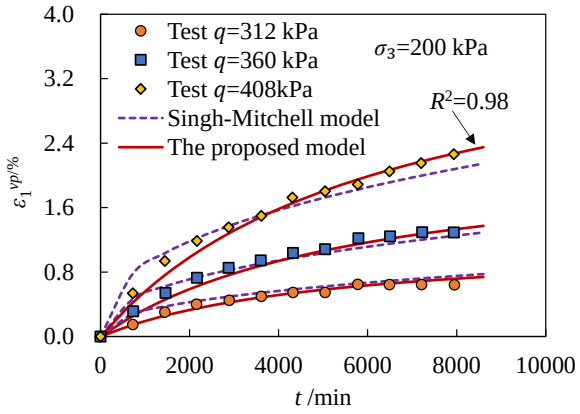

(a) Soft soils of Zhuhai, σ_3=200 kPa, q_f=480 kPa

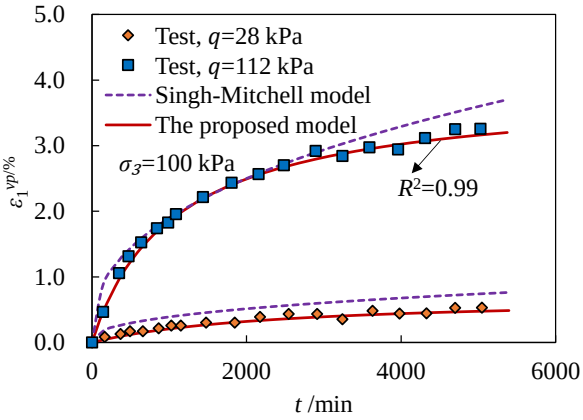

(b) Soft soils of Guangdong, σ_3=100 kPa, q_f=300 kPa

Fig. 12 Comparison of measured and computed strain

cannot describe the characteristics of first increase and then decrease.

$$\frac{\rho}{\rho_0} = aD_r + b \tag{19}$$

Where $D_r=(\sigma_1-\sigma_3)/(\sigma_1-\sigma_3)_f$ is shear stress level. ρ is the density of a clay. ρ_0 is the initial density of a clay. a, b are material parameters. a is the slope of a line in ρ/ρ_0- D_r plane. b is the relative density at shear stress level 0.

4.3 Comparison with Singh-Mitchell model

The creep values of soft clays of Guangdong and Zhuhai in laboratory tests are shown in Fig. 12. In the meantime, the creep values inferred from Singh-Mitchell model and the proposed model are given. In normal triaxial consolidation drainage test, Singh-Mitchell model can be written as Eq. (19).

$$\frac{d\varepsilon_1}{dt} = A_r \exp(\alpha D_r)(t_0/t)^m \tag{19}$$

Where A_r, α, m are material parameters. m is the slope of a line in $\ln(d\varepsilon_1/dt)$-$\ln t$ plane. A_r is the strain rate at shear stress level 0 and reference time t_0. Based on test data, values of three parameters of Zhuhai clays are A_r=-3.9E-6, α=5.08, m=1.41, and values of three parameters of Guangdong clays are A_r=-6.61E-5, α=5.85, m=1.4

Fig. 12 compares the test results with the calculated values of the two models. The results show that predictions of models are both very close to the experimental data. However, the calculations of the model proposed in this paper is closer to the test data, especially, at a lower or a high shear stress level. Studies have shown that the Singh-Mitchell model is suitable for the experimental results with shear stress levels of 20%-80%. Therefore, it is found from Fig. 12 that the Singh-Mitchell model is applicable no longer when the stress level is lower than 20%, such as soft clays of Guangdong at D_r=9.3%, or higher than 80%, such as soft clays of Zhuhai at D_r=85%. The model calculation results proposed in this paper are in good agreement with the laboratory data. The comparison results illustrate that the proposed model can more satisfactorily descried creep behaviour of soft clays in different shear stress levels, and the proposed creep model has better suitability.

5. Discussion

In recent years, various construction projects have developed rapidly. Due to the wide distribution of soft clays, the post-construction settlement of soft foundation has always been a topic of great concern to engineers. Therefore, it is necessary to predict post-construction settlement.

In this paper, the assumption that elastoplastic deformation and creep deformation are clearly divided is adopted. The method is easy to understand and master. Addresses the limitation of effective stress varying with time. The analysis and calculation of test data are simple. Clear physical meaning of model parameters is beneficial to engineering construction. However, it has to be admitted that this assumption has some limitations. It is possible that creep occurs in the primary consolidation period. However, most engineers focus on post-construction settlement. The primary consolidation stage of soft foundation of the buildings has been completed in the construction period. The post-construction settlement is dominated by the creep deformation stage assumed in this paper. Therefore, it is reasonable to divide creep and primary consolidation completely.

Of course, it is important to select the appropriate model in this process. Predictions of the proposed constitutive model of this paper and experimental data of different regions show close agreement. It is implied the proposed creep model has good suitability. However, there are still some shortcomings in the creep constitutive model proposed in this paper. The creep of soft clays has its own development characteristics. The flow surface equation of modified Cam-Clay model may be difficult to fully reflect the creep properties of soils, so the flow surface function of creep stage needs further to be studied.

6. Conclusions

In this paper, the creep volumetric strain behavior and creep model of soft clays are studied, the conclusions are as follows:

•The triaxial creep test data of soft clays indicated that, the strain-time curve showing in the ε-lg$t$ space can be divided into two lines with different slopes, and the time referring to the demarcation point is named as t_{EOP}. Therefore, the model is based on this simplification: when the loading time is before t_{EOP}, only the elastic and plastic strains occur, and can be predicted by MCC; when the time is after t_{EOP}, the soils has reached the creep stage, the strain occurs in this stage can be regarded as the creep components.

•The proposed hyperbolic equation expressing the relationship between creep volumetric strain, stress and time shows good applicability. Several triaxial creep test data of soft clays has verified that, it can well predict the creep volumetric strain under different confining pressures and different shear stress. Meanwhile, the 4 parameters can be determined easily by triaxial creep test data.

•The plastic flow law of the MCC model can be used as the creep flow law. On this basis, the expressions of the creep strain components are deduced, and are verified by successfully predicting the creep principal strains of various triaxial specimens. The sum of the deduced creep strain components and the elastic and plastic strain components in the MCC model can be regarded as the proposed creep model for soft clays.

References

Chen, B., Xu, Q. and Sun, D.A. (2014), "An elastoplastic model for structured clays", *Geomech. Eng*., **7**(2), 213-231. http://dx.doi.org/ 10.12989/gae.2014.7.2.213.

Chen, X.P., Huang, G.Y. and Liang, Z.S. (2003), "Study on soft properties of the pearl river delta", *Chinese J. Rock Mech. Eng*., 1,137-141. https://doi.org/1000-6915(2003)01-0137-05. (in Chinese).

Chen, Z.J., Feng, W.Q. and Yin, J.H. (2021), "A new simplified method for calculating short-term and long-term consolidation settlements of multi-layered soils considering creep limit", *Comput. Geotech*., **138**, 104324. https://doi.org/10.1016/j.compgeo.2021.104324.

Dong, W.J. (2007), "Study on the laboratory test of rheological characteristic of soft clay and long-term strength", Ph.D. Dissertation, Hohai University, Nanjing, Jiangsu, China.

Cai, Z.Y. *et al*. (2019), Geotechnical Test Method Standard. China Planning Press, Beijing, China.

Hawlader, B.C., Muhunthan, B. and Imai, G. (2003), "Viscosity effects on one-dimensional consolidation of clay", *Int. J. Geomech*., **3**(1), 99-110. https://doi.org/10.1061/(ASCE)1532-3641(2003)3:1(99).

Hessam, Y. and Mohammad, M.T. (2012), "Nonlinear consolidation of soft clays subjected to cyclic loading-part Ⅱ: verification and application", *Geomech. Eng*., **4**(4), 243-249. https://doi.org/ 10.12989/gae.2012.4.4.243.

Hu, J.L. (2013), "The study of creep characteristics for soft clay and its application on calculation of long-term subgrade settlement", Ph.D. Dissertation, Hohai University, Nanjing, Jiangsu, China.

Kim, D.K. (2005), "Comparisons of overstress theory with an empirical model in creep prediction for cohesive soils", *KSCE J. Civil Eng*., **9**(6), 489-494. https://doi.org/10.1007/bf02831485.

Krogsboll, A. (1998), "Constitutive model with time-dependent deformations", *Eng. Geol*., **49**(3-4), 285-292. https://doi.org/10.1016/s0013-7952(97)00060-4.

Lester, A.M., Kouretzis, G.P., Pineda, J.A. and Carter, J.P. (2021), "Finite element implementation of an isotach elastoplastic constitutive model for soft soils", *Comput. Geotech.*, **136**, 104248. https://doi.org/10.1016/j.compgeo.2021.10424.

Lin, H.D. and Wang, C.C. (1998), "Stress-strain-time function of clay", *J. Geotech. Geoenviron. Eng*., **124**(4), 289-296. https://doi.org/10.1061/(ASCE) 1090-0241(1998)124:4(289).

Liu, W.Z., Shi, Z.G., Zhang, J.H. and Zhang, D.W. (2019), "One-dimensional nonlinear consolidation behavior of structured soft clay under time-dependent loading", *Geomech. Eng*., **18**(3), 299-313. https://doi.org/ 10.12989/gae.2019.18.3.299.

Liu, Y.F. (2020), "Experimental study on consolidation rheological properties of Cangzhou coastal", Ph.D. Dissertation, North China University of Water Resources and Electric Power. Zhengzhou, Henan, China.

Mataic, I., Wang, D. and Korkiala-Tanttu, L. (2016), "Effect of destructuration on the compressibility of Perniö clay in incremental loading oedometer tests", *Int. J. Geomech*., **16**(1), 04015016. https://doi.org/10.1061/ (ASCE)GM.1943-5622.0000486.

Mesri, G. Eehres-Cordero, E. and Shields, D.R. (1981), "Shear stress-strain-time behaviour of clays", *Geoechnique*, **31**(4), 537-552. https://doi.org/10.1680/geot.1981.31.4.537.

Perzyna, P. (1966), "Fundamental problems in viscoplasticity", *Adv. Appl. Mech*., **9**(2), 243-377. https://doi.org/10.1016/S0065-2156(08)70009-7.

Roscoe, K.H. and Burland, JB. (1968), Engineering Plasticity, Cambridge University Press, Cambridge, England.

Singh, A. and Mitchell, J.K. (1968), "General stress-strain-time function for soils", *J. Soil Mech. Found. Div.*, **94**(1), 21-46. https://doi.org/10.1061/JSFEAQ. 0001084

Thu, M.L., Behzad, F., Hadi, K. and Sun, W.J. (2017), "Numerical optimization applying trust-region reflective least squares algorithm with constraints to optimize the non-linear creep parameters of soft soil", *Appl. Math. Model*., **41**, 236-256. https://doi.org/10.1016/j.apm.2016. 08.034.

Thu, M.L., Behzad, F., Mahdi, D. and Hadi, K. (2015), "Analyzing consolidation data to obtain elastic viscoplastic parameters of clay", *Geomech. Eng*., **8**(4), 559-594. https://doi.org/ 10.12989/gae.2015.8.4.559.

Vialov. (1987). Rheological principles of soil mechanics. Science Press, Beijing, China.

Xu, X.B. and Cui, Z.D. (2020), "Investigation of a fractional derivative creep model of clay and its numerical implementation", *Comput. Geotech*., **119**, 103387. https://doi.org/10.1016/j.compgeo.2019.103387.

Yin, J.H. and Graham, J. (1989), "Viscous-elastic-plastic modelling of one dimensional time-dependent behavior of clays", *Can. Geotech. J*., **26**, 199-209. https://doi.org/10.1139/t89-029.

Yin, J.H. and Graham, J. (1994), "Equivalent times and one-dimensional elastic visco-piastic modelling of time-dependent stress-strain behavior of clays", *Can. Geotech. J*., **31**, 42-52. https://doi.org/10.1016/0148-9062(94)90219-4.

Yin, J.H. and Graham, J. (1996), "Elastic visco-plastic modelling of one-dimensional consolidation", *Geotechnique*, **46**(3), 515-527. https://doi.org/10.1680/geot.1996.46.3.515.

Yin, J.H. and Graham, J. (1999), "Elastic visco-plastic modelling of the time-dependent stress-strain behavior of soils", *Can. Geotech. J*., **36**, 736-745. https://doi.org/10.1139/t99-042.

Yin, J.H. and Zhu, J.G. (1999), "Measured and predicted time-dependent stress-strain behavior of Hong Kong marine deposits", *Can. Geotech. J*., **36**, 760-766. https://doi.org/10.1139/t99-043.

Yin, J.H., Zhu, J.G. and Graham, J. (2002), "A new elastic visco-

plastic model for time-dependent behavior of normally and overconsolidated clays-theory and verification", *Can. Geotech. J.*, **39**(1), 157-173. https://doi.org/10.1139/ 01-074.

Yin, J.H. (2015), "Fundamental issues of elastic viscoplastic modeling of the time-dependent stress–strain behavior of geomaterials", *Int. J. Geomech*., **15**(5), A4015002. https://doi.org/10.1061/(ASCE)gm.1943-5622.0000485.

Zhao, T.B., Zhang, Y.B., Zhang, Q.Q. and Tan, Y.L. (2018), "Analysis on the creep response of bolted rock using bolted burgers model", *Geomech. Eng*., **14**(2), 141-149. https://10.12989/gae.2018.14.2.141.

Zhen, Y. Gang, L. Zhang, J. and Zhang, R. (2019), "Study on the creep behaviors of interactive marine-terrestrial deposit soils", *Adv. Civil Eng*., 1-14. https://doi.org/10.1155/2019/6042893.

Zhu, H.H., Chen, X.P. and Cheng, X.J. (2006), "Study on creep characteristics and model of soft soil considering drainage condition", *Rock Soil Mech*., **27**(5), 694-698. https://doi.org/10.16285/j.rsm.2006.05.003. (in Chinese)

Zhu, J.G. (2000), "Rheological behavior and elastic viscoplastic modelling of soil", Ph.D. Dissertation, The Hong Kong Polytechnic University, Hong Kong, China.

GC

Appendix A. Derivation of elastic strain increment

The elastic strain increment Eq. (A1) can be obtained from the generalized Hooke's law.

$$d\varepsilon_{ij}^{e} = \frac{1+\mu}{E}\frac{\kappa}{1+e_0} pd\sigma_{ij} - \frac{\mu}{(1-2\mu)}\frac{\kappa}{1+e_0} dp\delta_{ij} \tag{A1}$$

Where E is module of elasticity. μ is Poisson ratio. σ_{ij} represents the stress value under general stress state. δ_{ij} is a Kronecker symbol, when $i=j$, $\delta_{ij}=1$, otherwise 0. E is generally expressed as a function of the effective mean normal stress p in the modified Cam-Clay model, as Eq. (A2).

$$E = 3(1-2\mu)\frac{1+e_0}{\kappa} \tag{A2}$$

Where e_0 is initial void ratio. κ is the slope of the reloading curve after the rebound of the isotropic consolidation test in e, lnp-plane. From Eq. (A2), Eq. (A1) becomes Eq. (A3)

$$d\varepsilon_{ij}^{e} = \frac{1+\mu}{3(1-2\mu)}\frac{\kappa}{1+e_0} pd\sigma_{ij} - \frac{\mu}{(1-2\mu)}\frac{\kappa}{1+e_0} dp\delta_{ij} \tag{A3}$$

It is assumed the yield function is equal to plastic potential function with the employment of associated flow rule. According to the theory of plastic potential function, plastic incremental strain $d\varepsilon_{ij}^{p}$ is described by Eq. (A4).

$$\begin{aligned} d\varepsilon_{ij}^{p} &= d\chi\frac{dg}{d\sigma_{ij}} = \frac{\lambda-\kappa}{1+e_0} \\ &\left\{\frac{M^2p^2-q^2}{M^2p^2+q^2}\frac{\delta_{ij}}{3p} + \frac{3\left(\sigma_{ij}-p\delta_{ij}\right)}{M^2p^2+q^2}\right\} \\ &\left(dp + \frac{2pq}{M^2p^2-q^2}dq\right) \end{aligned} \tag{A4}$$

Appendix B.

The constitutive model

$$\begin{aligned} d\varepsilon_{ij} &= d\varepsilon_{ij}^{e} + d\varepsilon_{ij}^{p} + d\varepsilon_{ij}^{vp} \\ &= \frac{1+\mu}{3(1-2\mu)}\frac{\kappa}{1+e_0} pd\sigma_{ij} - \frac{\mu}{(1-2\mu)}\frac{\kappa}{1+e_0} dp\delta_{ij} \\ &+ \frac{\lambda-\kappa}{1+e_0}\left\{\frac{M^2p^2-q^2}{M^2p^2+q^2}\frac{\delta_{ij}}{3p} + \frac{3\left(\sigma_{ij}-p\delta_{ij}\right)}{M^2p^2+q^2}\right\} \\ &\left(dp + \frac{2pq}{M^2p^2-q^2}dq\right) \\ &+ \frac{\left[\frac{\delta_{ij}}{3} + \frac{3p\left(\sigma_{ij}-p\delta_{ij}\right)}{M^2p^2-q^2}\right]\left[1-\varepsilon_v^{vp}k_{v2}\left(\frac{q}{p}\right)^{-n_{v2}}\right]^2}{\left[k_{v1}\left(\frac{q}{p_a}\right)^{-n_{v1}}t_0\right]}dt \end{aligned} \tag{B1}$$

Major principal strain of creep strain

$$d\varepsilon_1^{vp} = \left[\frac{1}{3} + \frac{3p\left(\sigma_1-p\right)}{M^2p^2-q^2}\right]\frac{\left[1-\varepsilon_v^{vp}k_{v2}(q/p)^{-n_{v2}}\right]^2}{\left[k_{v1}(q/p_a)^{-n_{v1}}t_0\right]}dt \tag{B2}$$

Manor principal strain of creep strain

$$d\varepsilon_3^{vp} = \left[\frac{1}{3} + \frac{3p\left(\sigma_3-p\right)}{M^2p^2-q^2}\right]\frac{\left[1-\varepsilon_v^{vp}k_{v2}(q/p)^{-n_{v2}}\right]^2}{\left[k_{v1}(q/p_a)^{-n_{v1}}t_0\right]}dt \tag{B3}$$

Nomenclature

σ_1, σ_2, σ_3 effective major, intermediate, and minor principal stresses;
ε_1, ε_3 major and minor principal strains;
ε, ε^e, ε^p, ε^{vp} total, elastic, plastic and creep strains;
ε^{tp} the creep strain of the whole stage of consolidation;
p effective mean normal stress, $p = \dfrac{\sigma_1 + \sigma_2 + \sigma_3}{3}$;
q effective shear stress, $q = \dfrac{1}{\sqrt{2}}\sqrt{(\sigma_1 - \sigma_2)^2 + (\sigma_2 - \sigma_3)^2 + (\sigma_3 - \sigma_1)^2}$;
$\mathrm{d}\varepsilon_v^e$ increment in the elastic volumetric strain;
$\mathrm{d}\varepsilon_{ij}^e$ increment in the elastic strain;
ε_v^e elastic volumetric strain;
$\mathrm{d}\varepsilon_v^p$ increment in the plastic volumetric strain;
$\mathrm{d}\varepsilon_{ij}^p$ increment in the plastic strain;
ε_v^p plastic volumetric strain;
$\mathrm{d}\varepsilon_v^{vp}$ increment in the volumetric creep strain;
$\mathrm{d}\varepsilon_{ij}^{vp}$ increment in the creep strain;
ε_v^{vp} volumetric creep strain;
$\mathrm{d}\varepsilon_v$ increment in the volumetric strain;
κ slope of the reloading curve of the isotropic consolidation test in e-ln$p$ plane;
λ slope of the loading curve of the isotropic consolidation test in e-ln$p$ plane;
μ Poisson ratio;
T, t time of deformation and creep;
t_{EOP} time of primary consolidation;
E_s input energy during shearing;
G_s gravity density;
w water content;
w_l liquid limit;
w_p plastic limit;
e_0 initial void ratio;
ρ density;
ρ_d dry density;
M critical state stress ratio;
g plastic potential function;
f yield function;
Q creep strain rate flow surface function;
dS creep scaling function;
δ_{ij} Kronecker symbol;
χ parameter of the yield function;